THE ASTROPHYSICAL JOURNAL, 325:119–127, 1988 February 1

X-RAY SPECTRUM AND VARIABILITY OF THE BLACK HOLE CANDIDATE LMC X-3

A. TREVES,[1] T. BELLONI,[1] L. CHIAPPETTI,[2] L. MARASCHI,[1]
L. STELLA,[3,4], E. G. TANZI,[2] AND M. VAN DER KLIS[3]

Received 1987 February 2; accepted 1987 June 20

ABSTRACT

LMC X-3 was observed on seven occasions in 1983–1984 with the *EXOSAT* satellite covering various orbital phases. No phase related variability was detected, while the X-ray flux increased gradually by ~30% in two weeks. Analysis of the short term variability in terms of autocorrelation reveals a minimum time scale of 600 s, with an rms amplitude of ~1%. Energy spectra in the 0.3–9 keV range have been fitted with various analytical laws. A good fit is obtained with the Comptonization spectrum given by Sunyaev and Titarchuk, yielding an optical depth $\tau \sim 23$ and a temperature of ~1 keV. The results are compared with those of Cygnus X-1 in the low state and with the expectations of the standard accretion disk model.

Subject headings: black holes — radiation mechanisms — X-rays: binaries — X-rays: spectra

I. INTRODUCTION

LMC X-3 was discovered during a survey of the Large Magellanic Cloud with the *Uhuru* satellite (Leong *et al.* 1971). Its optical identification with a 16th magnitude star was proposed by Warren and Penfold (1975) on the basis of the error box determined with *Copernicus* (Rapley and Tuohy 1974). An important step forward in the understanding of the system was the discovery by Cowley *et al.* (1983) of the binary nature ($P = 1.7d$) of the proposed optical counterpart. The absence of optical emission from one component, whose mass, as indicated by the mass function, exceeds 9 $M_\odot$, and the association with a bright X-ray source made the system a very strong candidate for hosting a black hole. Mazeh *et al.* (1986) and McClintock (1986) further discuss the issue.

A list of pre-*EXOSAT* X-ray observations of the source is reported in Table 1, together with the measured flux at 2 keV. These observations demonstrated the large variability of the source, with no clear periodic pattern, and yielded spectral information indicating an unusually soft spectrum (White and Marshall 1984).

Here we report on a series of observations performed with *EXOSAT* in 1983 and 1984. Some preliminary results were presented in Treves *et al.* (1984). These are the first X-ray observations obtained after the discovery of the binary period, and the program was designed to include various orbital phases, with simultaneous optical coverage (see van Paradijs *et al.* 1987). The instrumentation on board of *EXOSAT* enables a study of the source in a wide spectral band, and rapid variability of the source can also be monitored.

The X-ray spectra are discussed in § II. The variability on a short time scale is discussed in § III. Astrophysical implications of the results are presented in § IV.

II. X-RAY SPECTRA

The source was observed with *EXOSAT* once in 1983 December and at six different epochs in 1984 November and December. A journal of the observations, together with the corresponding orbital phases calculated from the ephemeris given by van der Klis *et al.* (1985), is presented in Table 2. Here we consider the data deriving from the set of eight proportional counters filled with Argon, which are sensitive in the 1–15 keV range (medium-energy experiment), and from the channel multiplier array at the focus of a grazing incidence telescope (0.02–2.5 keV, low-energy experiment). A description of the instrumentation can be found in Taylor *et al.* (1981), de Korte, Bleeker, and den Boggende (1981), and Turner and Smith (1981).

a) *Medium-Energy Observations*

The medium-energy observations were carried out adopting the standard mode in which half of the experiment points at the source and the other half monitors the background. Before and after each observation, background data from the slew maneuver are available. The source intensity was between 37 and 50 counts s^{-1} $half^{-1}$ (1–9 keV); the background level in the same range was ~15 counts s^{-1} $half^{-1}$. As high solar activity hampered the ME data of 1984 December 12, only six observations are left for spectral analysis. For five of them the background remains steady, and, in order to construct spectra, the background measured in an experiment half during the slew was subtracted from the data obtained during the pointing at the source with the same half. The observation of 1984 December 23 showed irregular variation of the background: in this case, spectra integrated over 60 s were produced both for the on-source and offset half. The difference between the on- and off-source spectra was corrected channel by channel by the difference between the count rates of the two halves during the slew.

The source signal is detectable ($>5\sigma$) up to the PHA channel 34: the energy range adopted for spectral analysis is 1–9 keV (channels 5–34), restricted for some observations to 1–8 keV (channels 5–31) due to the poor statistics in the higher energy channels.

Within each observation the intensity and the hardness ratio (HR), defined as the ratio of the 4–8 keV to the 1–4 keV count rates, remain stable within 5% (see § III for a detailed timing analysis), but significant changes appear among different observations (see Table 2). A variation of 40% in flux is found in our set of observations. With respect to the recorded histori-

[1] Dipartimento di Fisica dell'Università, Milano, Italy.
[2] Istituto di Fisica Cosmica e Tecnologie Relative del CNR, Milano, Italy.
[3] Space Science Department of ESA, ESTEC, Noordwijk, The Netherlands.
[4] I.C.R.A. Dipartimento di Fisica "G. Marconi" dell'Università, Roma, Italy.

TABLE 1

THE RANGE OF X-RAY INTENSITY AT 2 keV FOR LMC X-3 AS MEASURED BY VARIOUS SATELLITES

Satellite	Instrument	Epoch	$F_{(2\ keV)}$ μJy	References
Uhuru	PC	1970 Dec–1973 Mar	32–94	1, 2
Copernicus	PC	1973 Mar–1974 Aug	35–176	3, 4
OSO 7	PC	1971 Dec–1973 Mar	45–107	5
SAS 3	RMC	...	<7–201	6, 7, 8
Ariel 5	EXP B	1974 Oct–1980 Mar	<1–197	9, 10
	EXP C	1977 Aug	66	11
HEAO 1	MC	1977 Aug–1978 Jan	23–185	12, 13
	EXP A-2	1977 Aug	17	14
Einstein	HRI	1978 Nov	...	15
	MPC	1978 Nov–1979 Apr	29–196	16
	SSS	1979 Jan	27	17
EXOSAT	ME	1983 Dec–1984 Dec	66–93	18

REFERENCES.—(1) Leong *et al.* 1971. (2) Forman *et al.* 1978. (3) Rapley and Tuohy 1974. (4) Tuohy and Rapley 1975. (5) Markert and Clark 1975. (6) Delvaille 1976. (7) Schnopper and Delvaille 1977. (8) Bradt and McClintock 1983. (9) Griffiths and Seward 1977. (10) McHardy *et al.* 1981. (11) Bell Burnell and Chiappetti 1984. (12) Johnston *et al.* 1978. (13) Johnston, Bradt, and Doxsey 1979. (14) Nugent *et al.* 1983. (15) Long, Helfand, and Grobelsky 1981. (16) Weisskopf *et al.* 1983. (17) White and Marshall 1984. (18) This paper.

cal variability (see Table 1) the X-ray state of the source appears intermediate. A gradual increase of ~30% is observed in 1984 December over 11 days. This corresponds to a brightening of the source in the optical band (van Paradijs *et al.* 1987). The HR correlates with the intensity: the spectrum hardens as the source brightens, as previously noted by Weisskopf *et al.* (1983). No correlation of the X-ray intensity with the orbital phase is found.

b) *Low-Energy Observations*

Each low-energy (LE) observation was performed by alternately using three different filters, namely aluminum/parylene, 3000 Å lexan, and boron (see Chiappetti and Davelaar [1984] for the effective areas). Images were produced by accumulating the data over the whole exposure time for each filter. The count rate was extracted from a box centered on the source by subtracting a position-dependent background. Standard corrections for dead time, point spread function, and vignetting effects were applied. The resulting count rates are reported in Table 2. The LE light curves with 60 s resolution showed no evidence of variability within each observation.

c) *The Combined Low-Energy and Medium-Energy Spectra*

The count rates in the three filters of the LE experiment can be treated as three additional channels and combined with the ME data in order to reconstruct the source spectra in the full energy range covered by the two experiments.

Various spectral models, as specified in the Appendix, were fitted to the data by means of the minimum χ^2 method. X-ray absorption was accounted for using the cross section of Brown and Gould (1970). The adopted errors for the count rates are the combination of the statistical errors with a fixed value of 1% taken to represent systematic errors in the ME response (Parmar and Smith 1985). The best-fitting parameters and the corresponding minimum χ^2 are reported in Table 3. It is apparent that the simplest spectral forms (thermal bremsstrahlung [TB], power law [PL], and blackbody [BB], which involve three free parameters (including N_H), yield unacceptable reduced chi-square values χ_r^2: 30–100 for PL or BB and 7–30 for the TB case. It is therefore necessary to consider more complex models.

The distortions to a blackbody distribution introduced by electron scattering can be approximately described by the expression designated as modified blackbody (MBB) in the Appendix (e.g., Rybicki and Lightman 1979). This contains an additional parameter, the gas density ρ, which, together with kT, determines the ratio between the Thomson scattering coefficient κ_{es} and the free-free absorption coefficient κ_{ff}. However, in the limit $\kappa_{ff} \ll \kappa_{es}$, which is nearly valid in the energy range in which we perform the fits, the additional parameter enters only as a normalization constant, and in some cases the uncertainty with which ρ can be determined is rather large. The values of χ_r^2 obtained with this type of model are nearly acceptable ($\chi_r^2 \sim 3$). The derived values of the column density ($N_H \sim 3 \times 10^{19}$ cm^{-2}) are lower than expected (see Table 3). In fact, the galactic column in the direction of LMC X-3, as derived from 21 cm surveys, is 2×10^{20} atoms cm^{-2}. Moreover, from the considerable local reddening deduced from the optical-ultraviolet spectrum (Treves *et al.* 1986), an additional column density $N_H = 10^{21}$ atoms cm^{-2} pertaining to LMC X-3 itself is obtained if the $N_H - A_V$ relation given by Bohlin (1975) is adopted.

The Comptonization of soft photons by electrons with $kT_e \ll m_e c^2$ and optical depth $\tau > 1$ is described analytically by the expression labeled Comptonization (C) in the Appendix, derived by Sunyaev and Titarchuk (1980). The free parameters in this case are globally four. Fits with this model yield acceptable χ_r^2 values and give a column density of $\sim 10^{21}$ atoms cm^{-2}, consistent with the total hydrogen column in front of the source. Examples of photon spectra reconstructed with the fitted model are given in Figure 1 for the two observations of 1984 December 15 and 26. Errors on the parameters were estimated computing χ^2 grids in the $\tau - kT_e$ plane for various fixed values of N_H. The projection in the $\tau - kT_e$ plane of the envelope of 90% confidence contours for each observation is reported in Figure 2. This is obtained with the $\Delta\chi^2 = 6.21$ corresponding to three interesting parameters (Lampton, Margon, and Bowyer 1976). The figure shows a flux increase and spectral hardening on 1984 December 15 and 26 of Table 2, which correspond to an increase in temperature and to a decrease of the optical depth. The variation of the parameters, though statistically significant, is rather small.

We also tried fits with two components using various combinations of thermal bremsstrahlung and blackbody distribu-

TABLE 2

OBSERVATIONS OF LMC X-3 WITH *EXOSAT*[a]

Start time (UT)		Start phase	Exposure time (s)	Count rate (counts s^{-1})	Hardness ratio
LE1 + 3000 Å Lexan Filter					
1983 Dec 11.....	01:16	0.54	2,331	0.582 ± 0.012	...
	06:47	0.69	2,731	...	...
1984 Nov 3.....	17:57	0.35	2,077	0.578 ± 0.011	...
	20:03	0.45	3,500	...	...
1984 Dec 12.....	16:29	0.20	3,653	0.631 ± 0.016	...
1984 Dec 15.....	05:39	0.68	2,620	0.619 ± 0.014	...
	09:00	0.77	1,415	...	...
1984 Dec 19.....	01:13	0.92	1,604	0.642 ± 0.014	...
	03:42	0.98	2,137	...	...
1984 Dec 23.....	04:47	0.36	2,614	0.711 ± 0.018	...
1984 Dec 26.....	12:17	0.31	2,391	0.694 ± 0.014	...
LE1 + Aluminum/Parylene Filter					
1983 Dec 11.....	03:33	0.60	7,324	0.371 ± 0.012	...
1984 Nov 3.....	18:35	0.37	2,250	0.426 ± 0.016	...
1984 Dec 12.....	15:25	0.16	3,620	0.497 ± 0.009	...
	18:41	0.24	4,227	...	...
1984 Dec 15.....	06:30	0.71	3,123	0.426 ± 0.010	...
	09:27	0.78	2,308	...	...
1984 Dec 19.....	01:44	0.93	2,176	0.451 ± 0.010	...
	04:21	0.00	2,596	...	...
1984 Dec 23.....	05:36	0.37	2,654	0.480 ± 0.014	...
	07:55	0.43	505	...	...
1984 Dec 26.....	13:06	0.32	2,081	0.470 ± 0.012	...
	14:58	0.37	1,993	...	...
LE1 + Boron Filter					
1983 Dec 11.....	02:24	0.57	3,098	0.208 ± 0.007	...
	05:43	0.65	3,644	...	...
1984 Nov 3.....	19:17	0.39	2,489	0.190 ± 0.011	...
1984 Dec 12.....	14:19	0.13	3,689	0.230 ± 0.007	...
	17:34	0.21	3,826	...	...
1984 Dec 15.....	07:25	0.73	3,260	0.214 ± 0.008	...
	10:09	0.80	1,483	...	...
1984 Dec 19.....	02:23	0.96	4,484	0.215 ± 0.006	...
1984 Dec 23.....	06:23	0.39	4,845	0.246 ± 0.007	...
	08:29	0.45	2,767	...	...
1984 Dec 26.....	13:43	0.34	2,042	0.272 ± 0.010	...
	15:35	0.38	2,018	...	...
ME Argon, 1–9 keV[b]					
1983 Dec 11.....	00:50	0.53	24,840	36.91 ± 0.04	0.2750 ± 0.0015
1984 Nov 3.....	17:16	0.33	12,080	36.09 ± 0.15	0.2708 ± 0.0037
1984 Dec 12.....	19:41	0.27	1,320	...	...
1984 Dec 15.....	05:03	0.67	17,980	39.68 ± 0.07	0.2669 ± 0.0017
1984 Dec 19.....	00:47	0.91	15,030	42.29 ± 0.08	0.2734 ± 0.0016
1984 Dec 23.....	04:24	0.34	16,500	48.21 ± 0.21	0.3090 ± 0.0043
1984 Dec 26.....	11:52	0.28	14,970	50.63 ± 0.09	0.3195 ± 0.0017

[a] Intensity measured with different filters for the LE experiment and in the 1–9 keV range for the ME experiment is given together with the hardness ratio of 4–8 keV to 1–4 keV. The statistical errors are indicated.

[b] Count rate is in counts per second per half.

tions. Despite the higher number (five) of free parameters, the superposition of two BBs does not give good fits or reasonable values of N_H, while the superposition of a TB and a BB distribution gives a good description of the observed spectra. The χ_r^2 values are acceptable, and the values of N_H are $\sim 9 \times 10^{20}$ atoms cm^{-2}, close to those obtained with the Comptonization fit. As in the case of low-mass X-ray binaries (LMXRBs) for which similar two component spectral fits have become widely used, the TB component has a higher luminosity than does the BB component. On the other hand, while in LMXRBs variability is usually associated with the BB component (White 1987), for LMC X-3 the flux increase is mainly due to the TB component.

III. SHORT-TERM VARIABILITY

During all the *EXOSAT* observations of LMC X-3, energy-resolved data from the ME Argon chambers (128 channels) were obtained with an accumulation time of 10 s. These data

1988ApJ...325..119T

TABLE 3

Day	PL	TB	BB	C	MBB	BB+BB	TB+BB
345 83	$N_H = 4.64 \times 10^{21}$	$N_H = 1.66 \times 10^{21}$	$N_H \leq 10^{19}$	$N_H = (0.75 - 0.86 - 1.00) \times 10^{21}$	$N_H = 2.87 \times 10^{19}$	$N_H \leq 10^{19}$	$N_H = 8.99 \times 10^{20}$
	α=2.81	kT=2.63	kT=0.75	kT=0.94–0.96–0.99	kT=1.12	kT_1=0.37	kT_{TB}=2.29
	$L = 7.73 \times 10^{38}$	$L = 3.28 \times 10^{38}$	$L = 1.72 \times 10^{38}$	τ=23.87–25.17–26.47	$\rho = 8.05 \times 10^{-6}$	kT_2=0.87	kT_{BB}=0.82
	χ^2_r=117.6 (30 d.o.f.)	χ^2_r=26.98 (30 d.o.f.)	χ^2_r=108.1 (30 d.o.f.)	$L = (2.67 - 2.76 - 2.88) \times 10^{38}$	$L = 2.09 \times 10^{38}$	$L_1 = 8.31 \times 10^{37}$	$L_{TB} = 1.99 \times 10^{38}$
				χ^2_r=2.70 (29 d.o.f.)	χ^2_r=5.18 (29 d.o.f.)	$L_2 = 1.30 \times 10^{38}$	$L_{BB} = 7.29 \times 10^{37}$
						χ^2_r=5.62 (28 d.o.f.)	χ^2_r=1.89 (28 d.o.f.)
308 84	$N_H = 3.59 \times 10^{21}$	$N_H = 1.45 \times 10^{21}$	$N_H \leq 10^{19}$	$N_H = (0.86 - 1.06 - 1.26) \times 10^{21}$	$N_H = 4.12 \times 10^{19}$	$N_H \leq 10^{19}$	$N_H = 7.29 \times 10^{20}$
	α=2.65	kT=2.70	kT=0.73	kT=0.95–0.99–1.03	kT=1.12	kT_1=0.41	kT_{TB}=2.95
	$L = 6.74 \times 10^{38}$	$L = 3.38 \times 10^{38}$	$L = 1.80 \times 10^{38}$	τ=22.09–23.94–26.07	$\rho = 6.07 \times 10^{-6}$	kT_2=0.94	kT_{BB}=0.72
	χ^2_r=30.57 (27 d.o.f.)	χ^2_r=6.68 (27 d.o.f.)	χ^2_r=62.98 (27 d.o.f.)	$L = (2.82 - 3.00 - 3.21) \times 10^{38}$	$L = 2.20 \times 10^{38}$	$L_1 = 1.03 \times 10^{38}$	$L_{TB} = 2.05 \times 10^{38}$
				χ^2_r=0.94 (26 d.o.f.)	χ^2_r=3.03 (26 d.o.f.)	$L_2 = 1.21 \times 10^{38}$	$L_{BB} = 6.88 \times 10^{37}$
						χ^2_r=5.63 (25 d.o.f.)	χ^2_r=0.43 (25 d.o.f.)
350 84	$N_H = 6.53 \times 10^{21}$	$N_H = 1.18 \times 10^{21}$	$N_H \leq 10^{19}$	$N_H = (0.69 - 0.80 - 0.92) \times 10^{21}$	$N_H = 3.40 \times 10^{19}$	$N_H \leq 10^{19}$	$N_H = 8.93 \times 10^{20}$
	α=2.86	kT=2.63	kT=0.75	kT=0.93–0.95–0.97	kT=1.13	kT_1=0.39	kT_{TB}=2.17
	$L = 9.17 \times 10^{38}$	$L = 3.70 \times 10^{38}$	$L = 1.94 \times 10^{38}$	τ=25.39–26.70–28.20	$\rho = 6.63 \times 10^{-6}$	kT_2=0.88	kT_{BB}=0.83
	χ^2_r=121.7 (30 d.o.f.)	χ^2_r=30.34 (30 d.o.f.)	χ^2_r=87.61 (30 d.o.f.)	$L = (2.87 - 2.98 - 3.09) \times 10^{38}$	$L = 2.34 \times 10^{38}$	$L_1 = 9.03 \times 10^{37}$	$L_{TB} = 2.10 \times 10^{38}$
				χ^2_r=0.97 (29 d.o.f.)	χ^2_r=2.99 (29 d.o.f.)	$L_2 = 1.44 \times 10^{38}$	$L_{BB} = 9.27 \times 10^{37}$
						χ^2_r=6.86 (28 d.o.f.)	χ^2_r=1.02 (28 d.o.f.)
354 84	$N_H = 5.84 \times 10^{21}$	$N_H = 1.76 \times 10^{21}$	$N_H \leq 10^{19}$	$N_H = (0.75 - 0.87 - 1.00) \times 10^{21}$	$N_H = 3.48 \times 10^{19}$	$N_H \leq 10^{19}$	$N_H = 7.91 \times 10^{20}$
	α=2.79	kT=2.72	kT=0.76	kT=0.94–0.96–0.99	kT=1.14	kT_1=0.39	kT_{TB}=2.48
	$L = 9.17 \times 10^{38}$	$L = 3.83 \times 10^{38}$	$L = 2.03 \times 10^{38}$	τ=24.89–26.24–27.65	$\rho = 1.45 \times 10^{-5}$	kT_2=0.89	kT_{BB}=0.81
	χ^2_r=116.1 (27 d.o.f.)	χ^2_r=29.21 (27 d.o.f.)	χ^2_r=100.8 (27 d.o.f.)	$L = (2.89 - 3.13 - 3.25) \times 10^{38}$	$L = 2.43 \times 10^{38}$	$L_1 = 9.34 \times 10^{37}$	$L_{TB} = 2.15 \times 10^{38}$
				χ^2_r=1.33 (26 d.o.f.)	χ^2_r=4.82 (26 d.o.f.)	$L_2 = 1.52 \times 10^{38}$	$L_{BB} = 9.75 \times 10^{37}$
						χ^2_r=8.65 (25 d.o.f.)	χ^2_r=1.01 (25 d.o.f.)
358 84	$N_H = 3.56 \times 10^{21}$	$N_H = 1.47 \times 10^{21}$	$N_H \leq 10^{19}$	$N_H = (0.84 - 1.13 - 1.26) \times 10^{21}$	$N_H = 2.61 \times 10^{19}$	$N_H \leq 10^{19}$	$N_H = 8.18 \times 10^{20}$
	α=2.51	kT=3.12	kT=0.77	kT=1.01–1.06–1.09	kT=1.18	kT_1=0.36	kT_{TB}=2.79
	$L = 7.60 \times 10^{38}$	$L = 4.28 \times 10^{38}$	$L = 2.31 \times 10^{38}$	τ=21.97–23.12–25.48	$\rho = 2.00 \times 10^{-8}$	kT_2=0.90	kT_{BB}=0.83
	χ^2_r=28.50 (27 d.o.f.)	χ^2_r=7.35 (27 d.o.f.)	χ^2_r=66.17 (27 d.o.f.)	$L = (3.63 - 3.90 - 4.04) \times 10^{38}$	$L = 2.79 \times 10^{38}$	$L_1 = 1.09 \times 10^{38}$	$L_{TB} = 2.73 \times 10^{38}$
				χ^2_r=0.86 (26 d.o.f.)	χ^2_r=4.24 (26 d.o.f.)	$L_2 = 1.86 \times 10^{38}$	$L_{BB} = 8.72 \times 10^{37}$
						χ^2_r=2.03 (25 d.o.f.)	χ^2_r=0.83 (25 d.o.f.)
361 84	$N_H = 4.73 \times 10^{21}$	$N_H = 1.90 \times 10^{21}$	$N_H \leq 10^{19}$	$N_H = (0.97 - 1.13 - 1.35) \times 10^{21}$	$N_H = 4.48 \times 10^{19}$	$N_H \leq 10^{19}$	$N_H = 9.51 \times 10^{20}$
	α=2.64	kT=2.99	kT=0.80	kT=1.02–1.04–1.08	kT=1.21	kT_1=0.39	kT_{TB}=2.71
	$L = 9.50 \times 10^{38}$	$L = 4.72 \times 10^{38}$	$L = 2.54 \times 10^{38}$	τ=22.76–24.60–25.58	$\rho = 1.90 \times 10^{-6}$	kT_2=0.93	kT_{BB}=0.85
	χ^2_r=104.1 (27 d.o.f.)	χ^2_r=25.95 (27 d.o.f.)	χ^2_r=111.4 (27 d.o.f.)	$L = (3.93 - 4.00 - 4.28) \times 10^{38}$	$L = 3.03 \times 10^{38}$	$L_1 = 1.16 \times 10^{38}$	$L_{TB} = 3.32 \times 10^{38}$
				χ^2_r=1.43 (26 d.o.f.)	χ^2_r=5.62 (29 d.o.f.)	$L_2 = 1.94 \times 10^{38}$	$L_{BB} = 1.08 \times 10^{38}$
						χ^2_r=3.81 (25 d.o.f.)	χ^2_r=1.38 (25 d.o.f.)

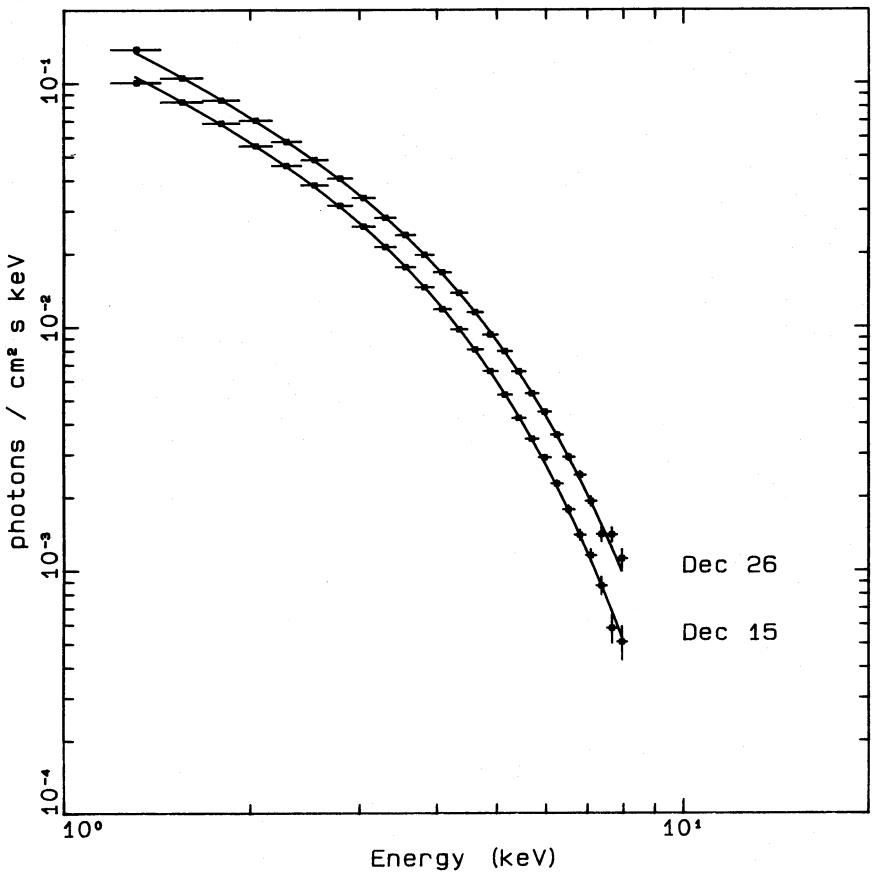

FIG. 1.—Reconstructed spectra with the Comptonization law for the observations of 1984 December 15 and 26

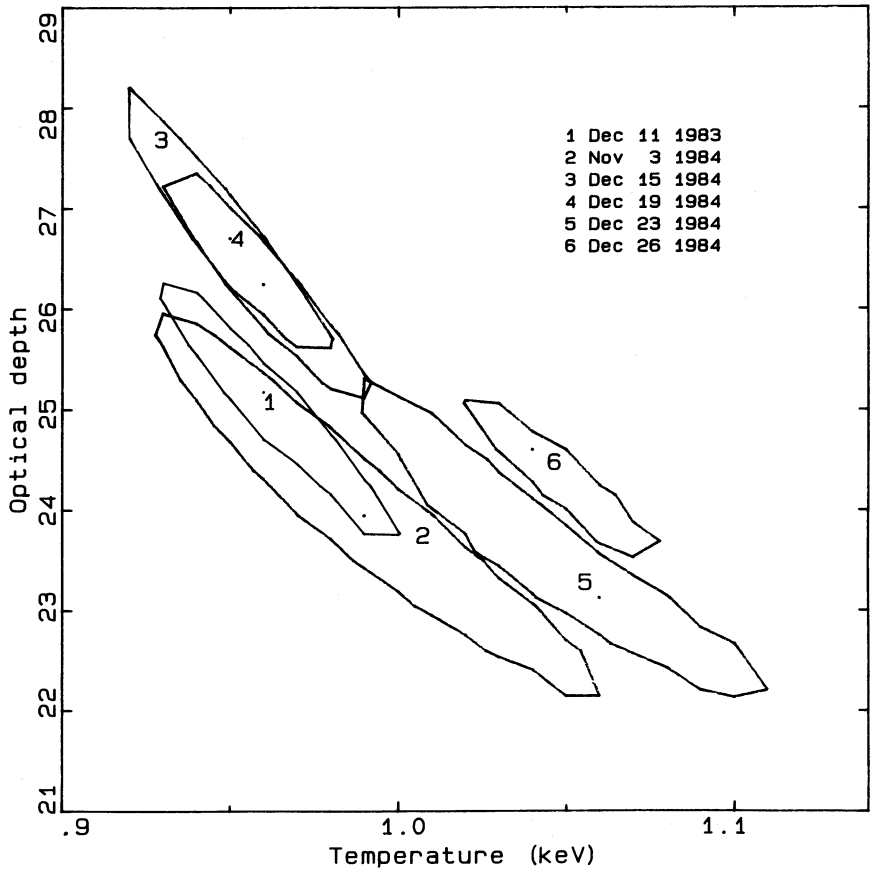

FIG. 2.—Projection of the 90% confidence contours in the $\tau - kT_e$ plane. Contours have been calculated with the $\Delta\chi^2$ corresponding to three interesting parameters (τ, kT_e, N_H; see text).

were analyzed to investigate the short-term activity of the source by accumulating 10 s and 50 s resolved light curves from the source in the 1–8 keV energy range. Particular attention was given to the removal of small amplitude fluctuations in the background. We first excluded all the intervals in which relatively large (>5%) background fluctuations were seen and subsequently analyzed for variability the 10 s and 50 s resolved background light curves from both the 1–8 keV range of the offset ME argon detectors (background A) and the 10–18 keV range of the ME argon detectors pointing at the source (background B; note that the source was not detected in the latter energy range). All the intervals in which the variance of the background data was found to be higher than the variance expected for a constant background (based on counting statistics and instrumental dead-time effects) were excluded from the source variability analysis. In this way we selected six intervals of 10,000–15,000 s duration from all but the 1984 December 23 observations. An example of a light curve is given in Figure 3. To investigate the source variability we computed the auto correlation function (ACF) by averaging the ACFs obtained for each of the six intervals resolved in 50 s bins (see Stella, Kahn, and Grindlay 1984). The results are given in the left panel of Figure 4.

The ACF shows an exponential-like decay with an *e*-folding time delay of ~ 600 s, revealing the presence of short-term variability on comparable time scales. The rms fractional variation of the activity of LMC X-3 over this time scale domain (evaluated from the ratio $\sigma/\bar{x}$, where σ^2 and $\bar{x}$ are, respectively, the source variance and average number of counts in the 50 s resolved light curves) was $1.2 \pm 0.3\%$ (uncertainty is 1 σ). This result cannot be ascribed to background fluctuations because the light curves of backgrounds A and B from the same six intervals showed no evidence for variability, with 95% confidence upper limits of 1.0% and 0.9% rms, respectively. On the contrary, if the 1.2% variability observed in LMC X-3 were to arise from background fluctuations, these should have had an rms variability of $\sim 4\%$. In addition, the ACFs of the background are consistent with zero correlation at any (nonzero) time lag, as expected from a white noise process. Instrumental effects can also be excluded. In particular, a 25 hr *EXOSAT* observation of the supernova remnant Cas A in 1984 July (which is a factor of ~ 3 brighter than LMC X-3 in the ME detectors) was analyzed by using the same technique. No evidence for variability was found with a 95% confidence upper limit of 0.4% rms over the same range of time scales.

The ACF of LMC X-3 is consistent with the exponential shape expected in a shot noise model consisting of Poisson-distributed exponential decay (or rise) shots, with a sharp rise (or decay) (see Sutherland, Weisskopf, and Kahn 1978). In this interpretation, the *e*-folding length of the ACF (~ 600 s) corresponds to the decay time of the shots. Due to poor statistics (in particular the third moment of the data could not be evaluated), the other shot noise model parameters of LMC X-3 could not be determined. Early modeling of the short-term activity of Cyg X-1 used the same approach (see Sutherland, Weisskopf, and Kahn 1978; Priedhorsky *et al.* 1979). The shot decay time deduced from Cyg X-1 was ~ 1 s. However, more recent investigations have shown that simple shot noise models do not adequately account for the variability properties of Cyg X-1, although a characteristic time scale of a few seconds is definitely present (for details see Nolan *et al.* 1981).

To allow an easy comparison with our LMC X-3 results, we calculated the ACF of a 10,000 s ME light curve of Cyg X-1 with 50 s resolution obtained by *EXOSAT* in 1985 August (a detailed study of the *EXOSAT* observations of Cyg X-1 will be reported elsewhere). Only the counts from two ME PHA channels around 2.5 keV were considered, in order to produce a rate of ~ 40 counts s^{-1}, similar to that of LMC X-3. The ACF is shown in the right panel of Figure 4. A pronounced spike

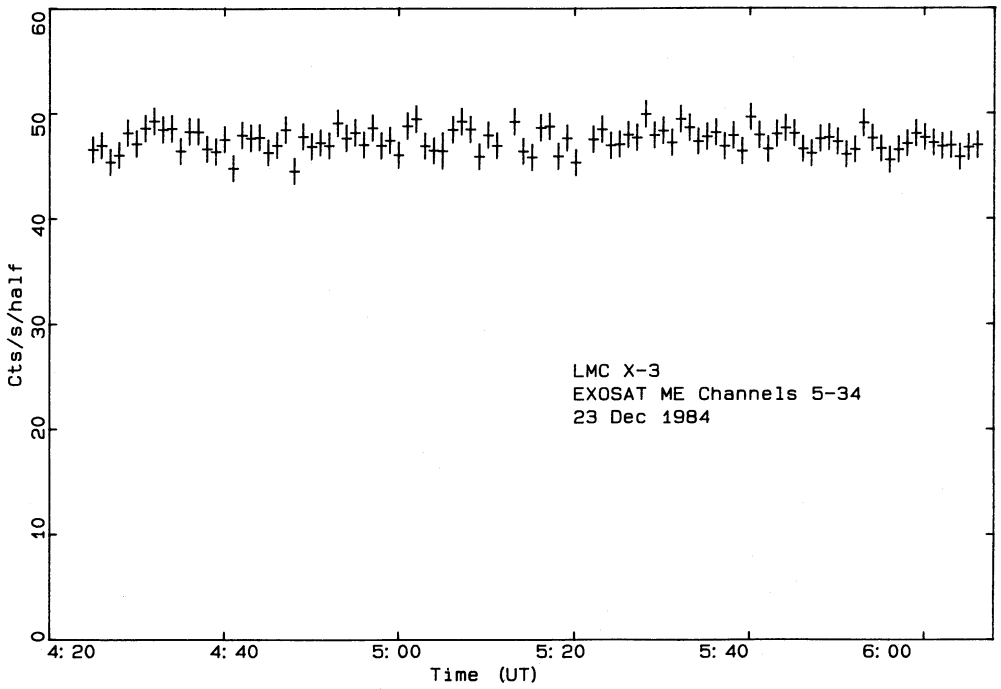

FIG. 3.—The ME light curve of LMC X-3 with 60 s bins for the observation of 1984 December 23

1988ApJ...325..119T

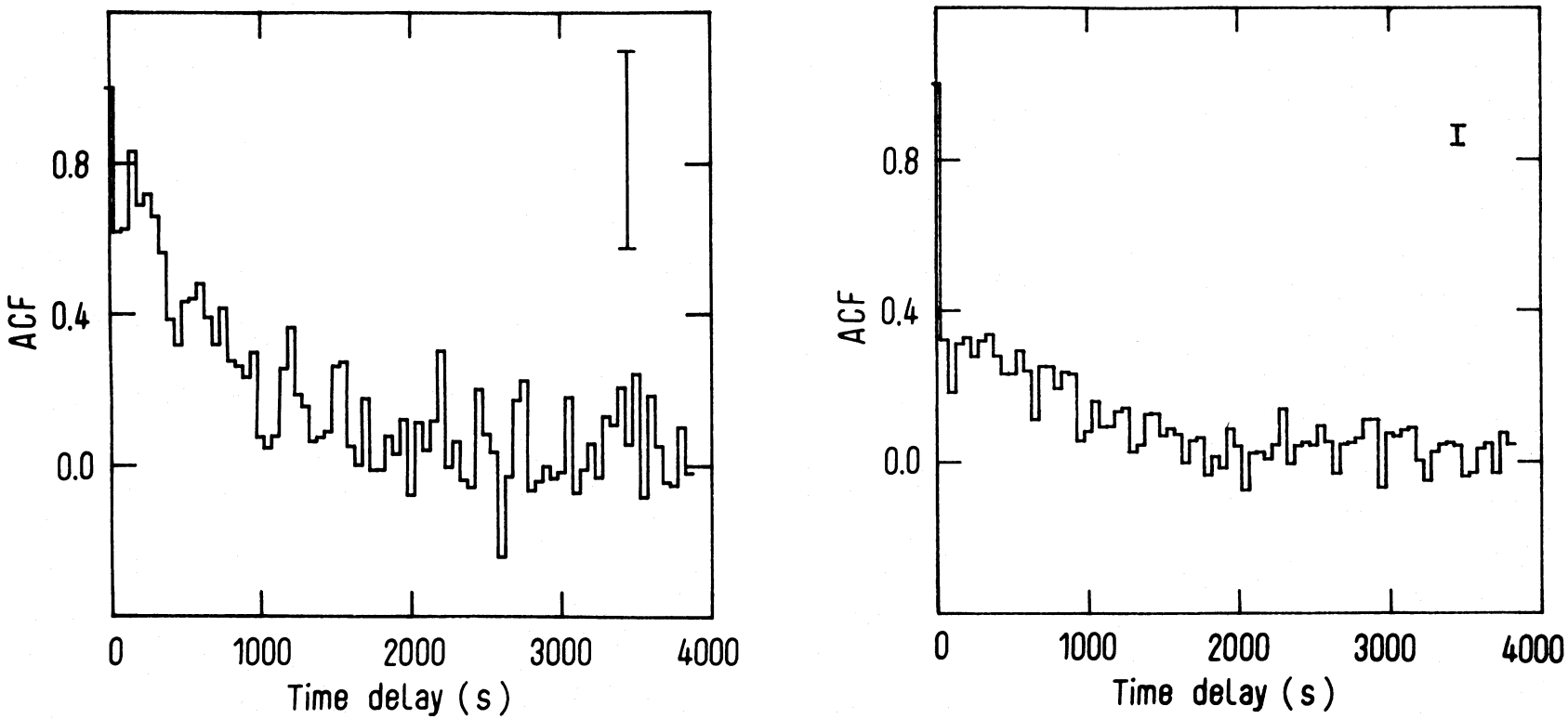

FIG. 4.—Autocorrelation function of the 50 s resolved ME light curves of LMC X-3 (*left panel*) and Cyg X-1 (*right panel*). The characteristic $\pm 1\ \sigma$ error bar is indicated in the upper right corner of each panel.

involving a jump of correlation of ~70% is seen at zero time lag, indicating that in the case of Cyg X-1 only about one-third of the variance measured in the 50 s binned light curve is actually resolved by the ACF. The zero lag spike is clearly a signature of the short-term activity of Cyg X-1 on time scales ≤50 s. In the ACF of LMC X-3 there is no evidence for such a spike. In particular, a 70% increase of correlation at zero time lag can be excluded at a confidence level of 97% in the case of LMC X-3. This confirms that the short-term variability properties of the two sources are different.

Therefore, the indication of our study is that LMC X-3 varies on time scales of ~600 s, several hundred times longer than the characteristic time scale for the variability of Cyg X-1. To firmly assess that the 600 s time scale is indeed a characteristic time scale of the variability of LMC X-3 requires an investigation of the source behavior over a wide range of time scales. Owing to poor statistics, the ACF analysis presented here fails when a light-curve resolution smaller than 50 s is used. However, since the rms variability of the Cyg X-1 50 s resolved light curve was ~8.5%, the conclusion can be reached that LMC X-3 is a factor of ~7 less variable than Cyg X-1 over the same range of time scales.

IV. DISCUSSION

The spectral shapes which are preferred on the basis of the low χ_r^2 and of the expected value of hydrogen column density (see § II) are the Comptonization of soft photons and the superposition of a thermal bremsstrahlung and a blackbody distributions. The TB + BB model was first introduced to account for the X-ray spectra of LMXRBs. The origin of the two components is not established, but a plausible interpretation is that one is associated with the inner parts of the accretion disk and the other with the neutron star's surface and/or with the boundary layer between the disk and the surface (White 1987). In applying the same model to the case of LMC X-3, the first important difference is the fact that no radiation is expected to emerge from the central region within the inner rim of the disk. The two components could be associated with the disk itself (BB) and to a corona around it (TB). The parameters derived for the BB component compare reasonably well with the size and temperature of the innermost region of the disk. However, the interpretation of the TB component encounters two difficulties. First, the emission measure, together with the condition that the emitting plasma be thin in the X-ray range ($h\nu_a < 0.5$ keV), requires that the radiating region be larger than 10^8 cm. Second, the fact that the TB component contains most of the luminosity implies that most of the energy dissipated in the inner disk is transported to a supposedly large corona. For these reasons, though it gives a good formal description of our data, we consider this TB + BB spectral model unrealistic for LMC X-3.

The Comptonized model was derived by Sunyaev and Titarchuk (1980) solving the Kompaneets equation for the stationary propagation of soft photons ($h\nu \ll kT$) through a spherical or planar electron cloud with constant density and temperature.

The parameters derived for LMC X-3 with this spectral model are $\tau \sim 23$, $kT_e \sim 1$ keV. A consistency problem arises because of the high optical depth and the relatively low temperature. In fact, the transparency frequency above which the medium becomes effectively thin is given by

$$h\nu_{\rm tr} = 0.46 h_6^{-1/2} \text{ keV} , \quad (1)$$

where h_6 is the depth of the emitting region in units of 10^6 cm. The ratio between kT and $h\nu_{\rm tr}$ is therefore $2h_6^{1/2}$, which is rather small. We suspect that the real physical conditions may be close to those of a partially Comptonized blackbody, for which an analytic representation is quite complicated and beyond the scope of this paper.

In the case of Cyg X-1 Sunyaev and Trümper (1979) fitted the low-state spectrum ($L \sim 10^{37}$ ergs s^{-1}) in the range 15–200 keV with the same Comptonization model deriving $\tau \sim 5$ and $kT \sim 27$ keV. For these values of the parameters, the scattering atmosphere is effectively transparent in the X-ray range and the model is self consistent. It is worth emphasizing that the derived Comptonization parameter

$$y = \frac{4kT}{m_e c^2} \tau^2 ,$$

which describes the energy transfer from electrons to photons, has the same value in the cases of both Cyg X-1 and LMC X-3.

Let us now compare the derived electron density and optical depth with those predicted by the standard theory of accretion disks. The high luminosity and low temperature of LMC X-3 indicate that the relevant regime is the one where radiation pressure dominates the gas pressure in the innermost region (Shakura and Sunyaev 1973). In this case, the inner disk temperature is given by

$$T = 1.4 \times 10^7 r_7^{-3/8} \alpha^{-1/4} \text{ K} , \quad (2)$$

independent of the accretion rate, and the optical depth by

$$\tau = 5\alpha^{-1} r_7^{3/2} \dot{m}^{-1} , \quad (3)$$

where r_7 is the distance in units of 10^7 cm and $\dot{m}$ is the accretion rate in units of 2×10^{19} g s^{-1}. With $L = 3 \times 10^{38}$ ergs s^{-1} and an efficiency of 6%, we obtain $\dot{m} \sim 0.3$. Therefore, the derived parameters of LMC X-3 can be reproduced by the disk model for $r_7 \sim 1$ and α close to 1.

However, the same disk model is clearly inadequate when applied to the case of Cyg X-1. In fact, given the lower luminosity, the relevant accretion rate should be smaller than that of LMC X-3 by at least a factor of 10. This, according to equation (3), would yield for Cyg X-1 a larger optical depth, contrary to the results of Sunyaev and Trümper. Moreover, no explanation for the higher temperature of Cyg X-1 can be found within this disk model.

The variability time scale is probably several hundred times longer in LMC X-3 than in Cyg X-1, and both are much larger than the dynamical time scale. If the fluctuations were associated with the thermal instability, the fact that the more luminous and cooler source has a longer time scale is in qualitative agreement with the theory (e.g., Pringle 1981; Abramowicz 1987).

In conclusion, our spectral results on LMC X-3 are satisfactorily fitted by the Sunyaev and Titarchuk Comptonization model, which was successfully introduced for accounting for the low state of Cyg X-1. We find the more luminous source, LMC X-3, to have higher optical depth and lower temperature with respect to Cyg X-1. This is inconsistent with the expectations of the classical Shakura and Sunyaev accretion disk model. We consider that this disagreement points to the inadequacy of the model of Shakura and Sunyaev for the radiation

pressure dominated region. In fact, in the other regions of the disk the optical thickness is an increasing function of the accretion rate (i.e., of the luminosity). On the other hand, the optical depths calculated in the other regimes are much larger than those derived from the spectral fits. The spectral results discussed above may be taken as a starting point for the development of new models.

We thank J. van Paradijs and K. Makishima for helpful comments.

APPENDIX

ANALYTICAL FORMS FITTED TO X-RAY SPECTRA

The spectral models which were fitted to the data are as follows:

Power law (PL)

$$\frac{dN}{dE} = N_0 A(N_H) E^{-\alpha} .$$

Thermal bremsstrahlung (TB)

$$\frac{dN}{dE} = N_0 A(N_H) g(E) \frac{1}{\sqrt{kT}} e^{-E/kT} , \qquad \text{where } g(E) = 0.8\left(\frac{E}{kT}\right)^{-0.4} .$$

Blackbody (BB)

$$\frac{dN}{dE} = N_0 A(N_H) \frac{E^2}{e^{E/kT} - 1} .$$

Comptonization (C)

$$\frac{dN}{dE} = N_0 A(N_H)\left(\frac{E}{kT_e}\right)^2 e^{-(E)/(kT_e)} \int_0^\infty d\mu e^{-\mu} \mu^{n-1}\left[1 + \mu\left(\frac{E}{kT_e}\right)^{-1}\right]^{n+3} , \qquad \text{where } n = -\frac{3}{2} + \sqrt{\gamma + \frac{9}{4}} , \qquad \gamma = \frac{\pi^2}{3} \frac{m_e c^2}{[(\tau + 2/3)^2 kT_e]} .$$

Modified blackbody (MBB)

$$\frac{dN}{dE} = N_0 A(N_H) \frac{E^2}{e^{E/kT} - 1} \sqrt{\frac{\kappa_{ff}}{\kappa_{ff} + \kappa_{es}}} , \qquad \text{where } \kappa_{es} = 0.4, \qquad \kappa_{ff} = 2.63\rho(kT)^{-7/2}(1 - e^{-E/kT})\left(\frac{E}{kT}\right)^{-3} .$$

REFERENCES

Abramowicz, M. A. 1987, in *Variability of Galactic and Extragalactic X-Ray Sources*, ed. A. Treves (Milano: Ass. Av. Astr.), p. 137.
Bell Burnell, S. J., and Chiappetti, L. 1984, *Astr. Ap. Suppl.*, **56**, 415.
Bohlin, R. C. 1975, *Ap. J.*, **200**, 402.
Bradt, H. V. V., and McClintock, J. E. 1983, *Ann. Rev. Astr. Ap.*, **21**, 13.
Brown, R. L., and Gould, J. 1970, *Phys. Rev. D*, **1**, 2252.
Chiappetti, L., and Davelaar, J. 1984, *EXOSAT Observers' Guide*, Vol. **3**, § 8.1.
Cowley, A. P., Crampton, D., Hutchings, J. B., Remillard, R., and Penfold, J. E. 1983, *Ap. J.*, **272**, 118.
de Korte, P. A. J., Bleeker, J. A. M., and den Boggende, A. F. J. 1981, *Space Sci. Rev.*, **30**, 495.
Delvaille, J. P. 1976, *IAU Circ.*, No. 2396.
Forman, W., Jones, C., Cominsky, L., Julien, P., Murray, S., Peters, G., Tananbaum, H., and Giacconi, R. 1978, *Ap. J. Suppl.*, **38**, 357.
Griffiths, R. E., and Seward, F. D. 1977, *M.N.R.A.S.*, **180**, 75p.
Johnston, M. D., Bradt, H. V., and Doxsey, R. E. 1979, *Ap. J.*, **233**, 514.
Johnston, M. D., Bradt, H. V., Doxsey, R. E., Gursky, H., Schwartz, D. A., Schwarz, J., and van Paradijs, J. 1978, *Ap. J. (Letters)*, **225**, L59.
Lampton, M., Margon, B., and Bowyer, S. 1976, *Ap. J.*, **208**, 177.
Leong, C., Kellogg, E., Gursky, H., Tananbaum, H., and Giacconi, R. 1971, *Ap. J. (Letters)*, **170**, L67.
Long, K. S., Helfand, D. J., and Grabelsky, D. A. 1981, *Ap. J.*, **248**, 925.
Markert, T. H., and Clark, G. W. 1975, *Ap. J. (Letters)*, **196**, L55.
McClintock, J. E. 1986, *Ap. J.*, **308**, 110.
McHardy, I. M., Lawrence, A., Pye, J. P., and Pounds, K. A. 1981, *M.N.R.A.S.*, **197**, 893.
Mazeh, T., van Paradijs, J., van den Heuvel, E. P. J., and Savonije, G. J. 1986, *Astr. Ap.*, **157**, 113.
Nolan, P. L., *et al.* 1981, *Ap. J.*, **246**, 494.
Nugent, J. J., *et al.* 1983, *Ap. J. Suppl.*, **51**, 1.
Parmar, A. N., and Smith, A. 1985, *EXOSAT Express*, **10**, 40.
Priedhorsky, W. C., Garmire, G. P., Rothschild, R. E., Boldt, E., Serlemitsos, P., and Holt, S. 1979, *Ap. J.*, **233**, 350.
Pringle, J. E. 1981, *Ann. Rev. Astr. Ap.*, **19**, 137.
Rapley, C. G., and Tuohy, I. R. 1974, *Ap. J. (Letters)*, **191**, L113.
Rybicki, G. B., and Lightman, A. P. 1979, *Radiative Processes in Astrophysics* (New York: Wiley).
Schnopper, H. W., and Delvaille, J. P. 1977, *Ann. NY Acad. Sci.*, **302**, 300.
Stella, L., Kahn, S. M., and Grindlay, J. E. 1984, *Ap. J.*, **282**, 713.
Shakura, N. I., and Sunyaev, R. A. 1973, *Astr. Ap.*, **24**, 337.
Sunyaev, R. A., and Titarchuk, L. G. 1980, *Astr. Ap.*, **86**, 121.
Sunyaev, R. A., and Trümper, J. 1979, *Nature*, **279**, 508.
Sutherland, P. G., Weisskopf, M. C., and Kahn, S. M. 1978, *Ap. J.*, **219**, 1029.
Taylor, B. G., Andresen, R. D., Peacock, A., and Zobl, R. 1981, *Space Sci. Rev.*, **30**, 479.
Treves, A., Belloni, T., Chiappetti, L., Cristiani, S., Falomo, R., Maraschi, L., Tanzi, E. G., and van der Klis, M. 1986, *ESA* SP-263, 451.
Treves, A., Bonnet Bidaud, J. M., Chiappetti, L., Maraschi, L., Stella, L., Tanzi, E. G., and van der Klis, M. 1984, in *X-Ray Astronomy*, ed. M. Oda and R. Giacconi (Tokyo: Inst. Space Astronautical Sci.), p. 259.
Tuohy, I. R., and Rapley, C. G. 1975, *Ap. J. (Letters)*, **198**, L69.
Turner, M. J. L., and Smith, A. 1981, *Space Sci. Rev.*, **30**, 513.
van der Klis, M., Clausen, J. V., Jensen, K., Tjemkes, S., and van Paradijs, J. 1985, *Astr. Ap.*, **151**, 322.
van Paradijs, J., *et al.* 1987, *Astr. Ap.*, **184**, 201.
Warren, P. R., and Penfold, J. E. 1975, *M.N.R.A.S.*, **172**, 41P.
Weisskopf, M. C., Kahn, S. M., Darbro, W. A., Elsner, W. A., Grindlay, J. E., Naranan, S., Sutherland, P. G., and Williams, A. G. 1983, *Ap. J. (Letters)*, **274**, L65.
White, N. E. 1987, in *Variability of Galactic and Extragalactic X-Ray Sources*, ed. A. Treves (Milano: Ass. Av. Astr.), p. 165.
White, N. E., and Marshall, F. E. 1984, *Ap. J.*, **281**, 354.

BELLONI, T., MARASCHI, L., and TREVES, A.: Sezione di Astrofisica, Dipartimento di Fisica dell'Università, Via Celoria 16, 20133 Milano, Italy

CHIAPPETTI, L., and TANZI, E. G.: Istituto di Fisica Cosmica e Tecnologie Relative del CNR, Via Bassini 15, 20133 Milano, Italy

STELLA, L., and VAN DER KLIS, M.: Space Science Department of ESA, ESTEC, Postbus 299, 220 AG, Nordwijk, The Netherlands